

2D Matryoshka Sentence Embeddings*

Xianming Li ♦, Zongxi Li ♦, Jing Li ♦†, Haoran Xie ♦, Qing Li ♦

♦ Department of Computing, The Hong Kong Polytechnic University, Hong Kong SAR

† Department of Computing and Decision Sciences, Lingnan University, Hong Kong SAR

xianming.li@connect.polyu.hk

jing-amelia.li@polyu.edu.hk

Abstract

Common approaches rely on fixed-length embedding vectors from language models as sentence embeddings for downstream tasks such as semantic textual similarity (STS). Such methods are limited in their flexibility due to unknown computational constraints and budgets across various applications. Matryoshka Representation Learning (MRL) (Kusupati et al., 2022) encodes information at finer granularities, i.e., with lower embedding dimensions, to adaptively accommodate *ad hoc* tasks. Similar accuracy can be achieved with a smaller embedding size, leading to speedups in downstream tasks. Despite its improved efficiency, MRL still requires traversing all Transformer layers before obtaining the embedding, which remains the dominant factor in time and memory consumption. This prompts consideration of whether the fixed number of Transformer layers affects representation quality and whether using intermediate layers for sentence representation is feasible. In this paper, we introduce a novel sentence embedding model called *Two-dimensional Matryoshka Sentence Embedding* (2DMSE)¹. It supports elastic settings for both embedding sizes and Transformer layers, offering greater flexibility and efficiency than MRL. We conduct extensive experiments on STS tasks and downstream applications. The experimental results demonstrate the effectiveness of our proposed model in dynamically supporting different embedding sizes and Transformer layers, allowing it to be highly adaptable to various scenarios.

1 Introduction

Sentence embedding learning (Conneau et al., 2017; Cer et al., 2018; Reimers and Gurevych, 2019; Gao et al., 2021; Li and Li, 2023a) is a fundamental task in semantic textual similarity (STS). It

captures essential semantic and syntactic information in language, playing a crucial role in various scenarios such as retrieval augmented generation (Gao et al., 2023) and semantic duplication removal (Li and Li, 2024). The conventional deployment pipeline consists of two steps: (1) the forward pass to compute the representation and (2) the utilization of representations in downstream tasks (Kusupati et al., 2022).

Existing works (Reimers and Gurevych, 2019; Gao et al., 2021; Li and Li, 2023a, *inter alia*) commonly select the last Transformer layer with full hidden size for all tasks, regardless of varying resources and requirements. However, Kusupati et al. (2022) argues that using full-capacity embedding in such methods leads to unnecessary computational redundancy, as deep learning models tend to diffuse information, which could be encoded with fewer bits, across the high-dimensional vector. To inject elasticity and scalability into representation dimensions, Kusupati et al. (2022) proposed Matryoshka Representation Learning (MRL). MRL derives information-rich low-dimensional vectors from the same high-dimensional representation in a nested fashion, resembling human perception of the natural world (Hegde, 2008). Given one pretrained language model, MRL yields a set of coarse-to-fine-grained representations while preserving main semantics. With up to a $14\times$ reduction in embedding dimensions, MRL achieves speedup in step (2) tasks such as classification and retrieval.

However, it is important to note that MRL is only scalable to the embedding of the last Transformer layer. Despite providing efficiency for downstream applications, MRL incurs an expensive and constant inference stage, i.e., step (1) for calculating full-throughput embedding vectors at all layers, as the forward-pass pipeline remains unchanged. This imposes a high computational requirement for deploying MRL, particularly when the encoding model is relatively large. Moreover, we examined

Preprint. Work in progress.

† Corresponding author

¹Our code is available at https://github.com/SeanLee97/Angle/blob/main/README_2DMSE.md.

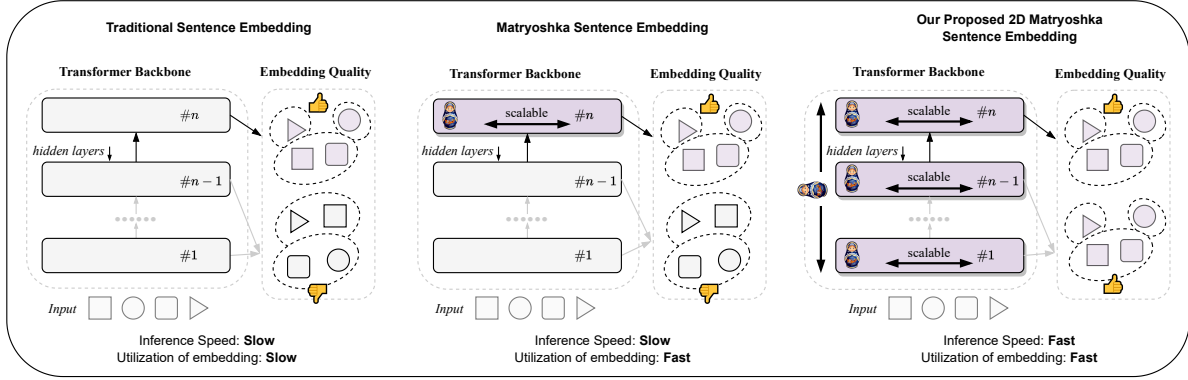


Figure 1: A visual comparison of various sentence embedding methods. The gray blocks represent Transformer layers fine-tuned with AnglE, which are not optimized for matryoshka representation. The purple block represents Transformer layers fine-tuned with AnglE together with matryoshka loss.

STS performance using embedding vectors from shallow layers of $\text{BERT}_{\text{base}}$ finetuned by AnglE² (Li and Li, 2023a), the state-of-the-art sentence embedding learning method, and observed unexpected performance drops from intermediate layers. These observations inspired us to further study representation capacity from another dimension: the depth of Transformer layers, in addition to the embedding size.

In this paper, we introduce the Two-dimensional Matryoshka Sentence Embedding \mathfrak{M}^2 (2DMSE). Given a pretrained language model, 2DMSE aims to extend the original MRL’s flexibility in sentence embedding learning by improving representation capacity at shallow layers. At each training step, we randomly sample a layer from the Transformer backbone (except for the last layer) following a uniform distribution. The proposed 2DMSE finetunes the last layer’s embedding and the sampled layer’s embedding simultaneously and in the matryoshka style for sentence embedding learning. Moreover, to further enhance the performance of shallow layers, we align their embeddings with those of the last layer for self-supervision, also following the matryoshka principle, by minimizing their Kullback-Leibler divergence. In this framework, shallow layers are explicitly involved in the representation learning process and are trained to become as powerful as the last layer. Therefore, every shallow layer is expected to be comparable with its subsequent layer, achieving a layer-level matryoshka effect through the continual pipeline. The key differences between the traditional sen-

tence embedding approach, Matryoshka sentence embedding, and our proposed 2DMSE are depicted in Figure 1.

2DMSE offers several advantages in sentence embedding learning. First, it significantly improves the performance of shallow layers’ embeddings on STS benchmarks. The shallow layers’ embeddings can already achieve acceptable performance, and substantial improvements are observed over the full-capacity embeddings, even without using additional training samples. Furthermore, the two-dimensional matryoshka training strategy makes the embedding model scalable and, most importantly, truncatable at two dimensions, i.e., the model depth and the embedding size, which can significantly enhance the efficiency and flexibility of utilizing 2DMSE embeddings. Given a large-scale language model, one can customize their Matryoshka models at different scales with a specified number of layers and embedding size according to the environment’s requirements and computational resources of an *ad hoc* task. Remarkably, the smaller models derived from 2DMSE can outperform their independently trained counterparts.

In summary, our contributions are as follows:

- We propose the Two-dimensional Matryoshka Sentence Embedding \mathfrak{M}^2 (2DMSE) framework for flexible and scalable sentence embedding learning.
- 2DMSE supports elastic configurations for both model depth and embedding size with marginal overhead and seamlessly adapts to different deployment requirements.
- Extensive experiments suggest that 2DMSE outperforms powerful baselines and demonstrates excellent scalability.

²We use $\text{BERT}_{\text{base}}$ as the base model in this work. For concise expression, we will use AnglE to denote the base model finetuned by AnglE. MRL and the proposed 2DMSE also use AnglE for sentence embedding learning.

2 Related Work

Our work focuses on embedding learning, specifically in the context of sentence embeddings. While early efforts focused primarily on word embeddings (Mikolov et al., 2013), sentence embeddings allow for semantic representation with richer contextual information. To better learn sentence embeddings, **supervised approaches** (Conneau et al., 2017; Cer et al., 2018; Reimers and Gurevych, 2019; Li and Li, 2023a) aligned with human supervision, thereby improving sentence embedding quality. Recently, **contrastive learning** techniques (Carlsson et al., 2020; Zhang et al., 2020; Giorgi et al., 2021; Gao et al., 2021; Yan et al., 2021; Chuang et al., 2022; Jiang et al., 2022; Zhuo et al., 2023; Xu et al., 2023) were used to improve sentence embeddings further with in-batch negative learning. With the advent of LLMs (OpenAI, 2022; Touvron et al., 2023), more and more **LLM-based** works have been proposed (Li and Li, 2023a,b; Wang et al., 2023) for boosting sentence embeddings significantly.

Most existing works in sentence embedding learning perform under a fixed setting, using full layers and embeddings, which limits scalability. To address this issue, a recent approach called Matryoshka Representation Learning (MRL) has been introduced, which allows for dynamic embedding sizes (Kusupati et al., 2022). However, while dynamic embedding size benefits downstream applications, it does not reduce computational overhead. To overcome this limitation, we propose 2D Matryoshka Sentence Embeddings (2DMSE). 2DMSE supports elastic settings for both embedding sizes and Transformer layers, offering greater flexibility and efficiency than MRL. It can be scaled down to smaller models with only a slight decrease in performance. It also effectively reduces computational overhead by choosing shallow layers. Its dynamic layer and embedding size make it highly versatile for various downstream applications.

3 2D Matryoshka Sentence Embeddings Framework

This section elaborates on the proposed 2DMSE. The overall framework is depicted in Figure 2. We introduce the encoder backbone in Section 3.1 and describe scalable sentence embedding learning in Section 3.2, followed by sentence embedding alignment in Section 3.3. We present the joint learning strategy for embedding optimization in Section 3.4.

3.1 Encoder

We use the pretrained language model as an encoder to transform the text into dense sentence embeddings. In this work, we use BERT_{base} (Devlin et al., 2019) as the backbone to encode text x as follows:

$$\mathbf{X}_n^d = \text{BERT}_{1:n}^{cls}(x)_{1:d} \in \mathbb{R}^d, \quad (1)$$

where cls stands for the pooling strategy; we adopt the ‘‘CLS’’ embeddings as the sentence embeddings following previous works (Gao et al., 2021; Li and Li, 2023a). $n \in [1, N]$ denotes the n -th layer of the N -layer Transformer backbone, and $d \in [1, D]$ represents the first d dimensions in the N -dimensional embeddings. n and d largely determine the size of an encoder model, suggesting two degrees of freedom. They allow scaling the encoder model in two dimensions: the number of layers and the embedding size, which are the basis for the proposed 2DMSE.

3.2 Scalable Sentence Embedding Learning

Following conventional approaches (Reimers and Gurevych, 2019; Gao et al., 2021; Li and Li, 2023a), we consistently train full-capacity embeddings from the last attention layer, \mathbf{X}_N^D , to ensure sentence embedding quality. The objective is as follows:

$$\mathcal{L}_N^D = \text{loss}(\mathbf{X}_N^D; A), \quad (2)$$

where $\text{loss}(\cdot)$ can be any loss function for sentence embedding learning, such as contrastive loss (Gao et al., 2021) or AnglE loss (Li and Li, 2023a). A is the auxiliary information used for loss computation, such as indication for positive or negative samples or ranking information.

Within the same training step, we randomly select a shallower Transformer layer following a uniform distribution and use its full embedding vector directly for representation learning:

$$\begin{aligned} \mathcal{L}_n^D &= \text{loss}(\mathbf{X}_n^D; A) \\ n &\sim \mathcal{U}(1, N-1), \end{aligned} \quad (3)$$

where $n \in [1, N]$ is the selected attention layer, and \mathcal{U} denotes the uniform distribution.

To achieve scalable representation learning in 2DMSE, we apply MRL (Kusupati et al., 2022) to train nested low-dimensional vectors at both the last layer, \mathbf{X}_N :

$$\begin{aligned} \mathcal{L}_N^d &= \text{loss}(\mathbf{X}_N^d; A) \\ d &\sim \mathcal{U}(1, D-1), \end{aligned} \quad (4)$$

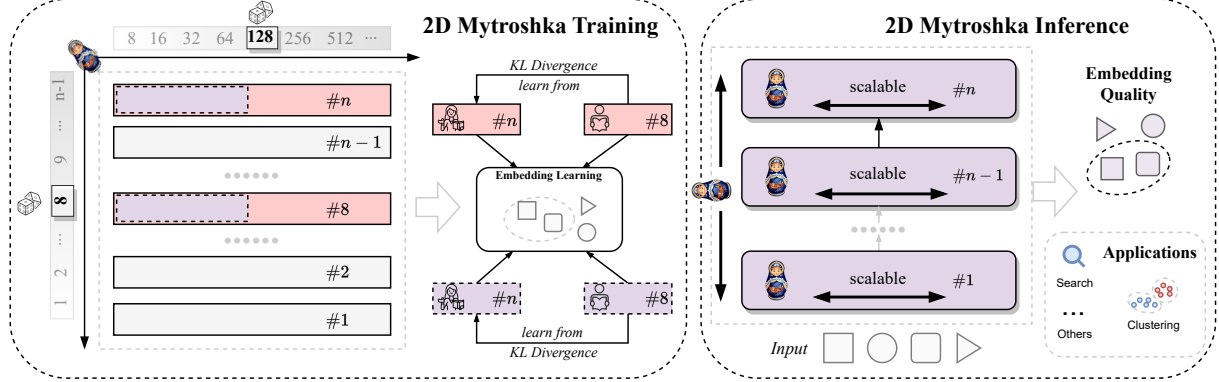


Figure 2: The overall framework of 2DMSE ². The left box represents the 2DMSE training stage, which involves two random processes: sampling a Transformer layer and sampling a hidden size. The selected layer and the last layer (pink rectangle) are then chosen for sentence embedding learning without scaling the hidden size. The selection of the hidden size (purple dashed rectangle) is also considered for sentence embedding learning. KL divergence is optimized during training to align the shallow layers with the last layer. The right box illustrates the inference stage, where all Transformer layers are scalable and can produce high-quality sentence embeddings for downstream applications after 2DMSE training.

and the sampled layer, \mathbf{X}_n :

$$\mathcal{L}_n^d = \text{loss}(\mathbf{X}_n^d; A), \quad (5)$$

where $d \in \mathbb{N}$ is the MRL embedding size and is sampled from a set of representation sizes $\mathcal{D} \subseteq [1, D - 1]$. To handle various embedding dimensions efficiently, we use the geometric series with a base of 8 and a ratio of 2 for \mathcal{D} .

3.3 Sentence Embedding Alignment \rightarrow

In addition to \mathcal{L}_N^D , \mathcal{L}_n^D , \mathcal{L}_N^d , and \mathcal{L}_n^d , we adopt distribution alignment to further improve embedding performance. According to the scaling law (Kaplan et al., 2020), more Transformer layers have more powerful language understanding capabilities. Following this law, we align the sampled shallow layer’s sentence embeddings to the last layer, thereby improving the shallow layer’s performance, by minimizing their divergence:

$$\mathcal{L}_{align} = \text{KLDiv}(\mathcal{L}_n^D, \mathcal{L}_N^D) + \text{KLDiv}(\mathcal{L}_n^d, \mathcal{L}_N^d), \quad (6)$$

where $\text{KLDiv}(q, p)$ denotes the Kullback-Leibler divergence, q is the prediction, p is the target.

3.4 Joint Learning

In the end, we add up all training objectives to compose the final objective as follows:

$$\mathcal{L} = \sum_L^S \lambda_L L, \quad (7)$$

where $S = \{\mathcal{L}_N^D, \mathcal{L}_n^D, \mathcal{L}_N^d, \mathcal{L}_n^d, \mathcal{L}_{align}\}$ stands for the objective set. Hyperparameter λ_L is the weight for objective L .

4 Experimental Setup

Datasets. We train the proposed 2DMSE on MultiNLI (Williams et al., 2018) and SNLI (Bowman et al., 2015) datasets following previous studies and evaluate its performance on the standard STS benchmark. This benchmark comprises seven widely adopted STS datasets: STS 2012-2016 (Agirre et al., 2012, 2013, 2014, 2015, 2016), SICK-R (Marelli et al., 2014), and STS-B (Cer et al., 2017).

Evaluation Metrics. We report Spearman’s correlation coefficient, following previous studies, for a fair comparison. We compute Spearman’s correlation using the SentEval toolkit (Conneau and Kiela, 2018) and present the results in the “all” setting.

Baselines. We primarily compare the proposed 2DMSE model with the MRL model (Kusupati et al., 2022) to demonstrate scalability. Additionally, to showcase overall effectiveness, we compare the proposed 2DMSE model with widely adopted baselines: InferSent (Conneau et al., 2017), USE (Cer et al., 2018), SBERT (Reimers and Gurevych, 2019), SimCSE (Gao et al., 2021), and the prior STS state-of-the-art (SOTA) AnglE (Li and Li, 2023a).

Implementation Details. For consistency, we utilize BERT_{base} (uncased) as the backbone for all baselines. As AnglE (Li and Li, 2023a) has demonstrated strong performance on STS tasks, we

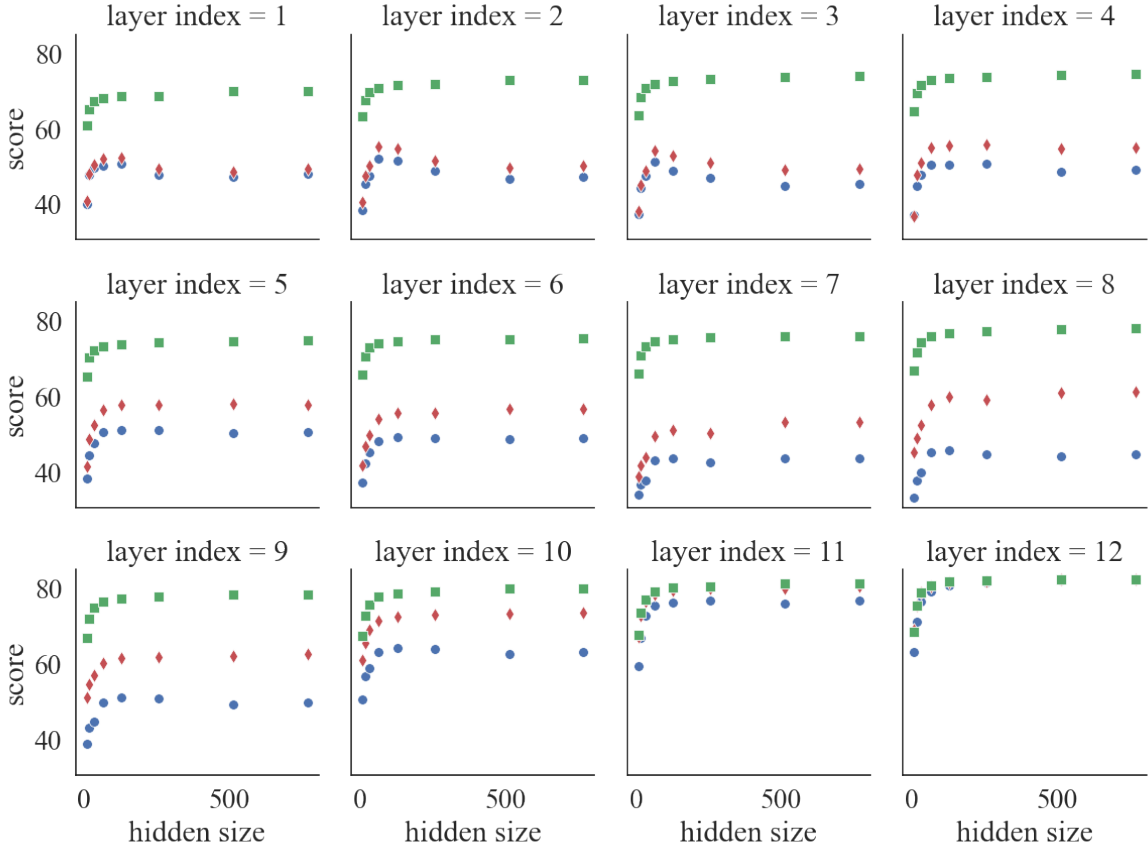


Figure 3: Results of the STS benchmark with a cascade of hidden sizes: $8 \rightarrow 16 \rightarrow 32 \rightarrow 64 \rightarrow 128 \rightarrow 256 \rightarrow 512 \rightarrow 768$ from $\text{BERT}_{\text{base}}$. The score represents the average Spearman’s correlation. $\text{BERT}_{\text{base}}$ serves as the backbone for all models. The blue \bullet indicates the results of sentence embeddings from AnglE without any scalable sentence embedding learning. The red \blacklozenge represents the results of matryoshka sentence embeddings. The green \blacksquare denotes the results of our proposed 2D Matryoshka Sentence Embeddings (2DMSE). The layer index = i denotes the i -th attention layer.

adopt its objective as the default loss function for sentence embedding learning. The initial learning rate is set to $5e-5$, following common practices. Other hyperparameters are set following Angle’s conventions. To ensure fair comparison, we fix the random seed to 42 for all experiments.

5 Experimental Results

We discuss the main STS benchmark results in Section 5.1. The ablation study investigating the significance of each component is reported in Section 5.2. Furthermore, we perform an efficiency study in Section 5.3 to quantify the speedup of 2DMSE in the inference stage.

5.1 Main Results

In the main experiments, we extract the matryoshka embedding vectors of every Transformer layer from the $\text{BERT}_{\text{base}}$ backbones that are finetuned by An-

gle (blue \bullet), AnglE with MRL (red \blacklozenge), and AnglE with our proposed 2DMSE (green \blacksquare) and test their performance on the standard STS benchmarks. For each layer, we adopt cascading vector dimensions of $\mathcal{D} = \{8, 16, 32, 64, 128, 256, 512, 768\}$.

The dimension-wise results of all layers are visualized as dot plots in Figure 3. Layer-wise results are presented in Figure 4b. Detailed results of each STS task are reported in Table 4, in Appendix A. We also compare with strong baselines for sentence embeddings and report the results in Table 1.

From both Figures 3 and 4b, it is evident that the proposed 2DMSE can significantly improve the embedding quality of shallow Transformer layers compared to MRL. Although all the models achieve comparable results with the full-capacity embeddings from the last layer, AnglE and MRL yield inferior performance in the shallow layers and even show performance fluctuations as lay-

Model	STS12	STS13	STS14	STS15	STS16	STS-B	SICK-R	Avg.
GloVe (Reimers and Gurevych, 2019)	52.86	66.75	62.15	72.77	66.87	68.03	65.65	65.01
USE (Reimers and Gurevych, 2019)	64.49	67.80	64.61	76.83	73.18	74.92	76.69	71.22
SBERT (Reimers and Gurevych, 2019)	70.97	76.53	73.19	79.09	74.30	77.03	72.91	74.89
SimCSE (Gao et al., 2021)	75.30	84.67	80.19	85.40	80.82	84.25	80.39	81.57
AnglE (Li and Li, 2023a)	75.09	85.56	80.66	86.44	82.47	85.16	81.23	82.37
MRL ($d = 768$) \star	75.72	86.79	81.89	86.91	81.74	85.50	79.44	82.57
2DMSE ($n = 12, d = 768$)	75.00	86.69	82.30	86.50	82.09	85.79	80.18	82.65

Table 1: Full-capacity sentence embedding performance on the standard STS benchmark. Results \star denote our implementation. BERT_{base} serves as the backbone for all models.

ers deepen. For example, AnglE achieves performance higher than 60.00 at the eighth layer, while MRL requires ten layers to reach 60.00. In contrast, 2DMSE achieves a score of 70.09 in the first Transformer layer and consistently improves until the last layer with a score of 82.65. These results indicate that 2DMSE equips each Transformer layer with promising embedding capacity, making it feasible to use the embedding vectors from shallow layers as sentence embeddings.

Furthermore, 2DMSE extends the flexibility and multifidelity of matryoshka learning to all layers. From Figure 3, 2DMSE produces rapid and stable performance improvements as the embedding dimension cascadingly grows. Such improvements are consistent across all layers, regardless of how the original embedding behaves, benefiting from the explicit optimization on the shallow layers. These results imply that one can utilize low-dimensional embedding vectors from intermediate layers while enjoying high embedding quality, signifying the considerable efficiency of 2DMSE in downstream tasks.

We compare 2DMSE with strong STS baselines using full-capacity sentence embedding ($n = 12, d = 768$) to test the absolute performance. Remarkably, 2DMSE outperforms these baselines. Both MRL and 2DMSE outperform the models finetuned with AnglE only, suggesting that matryoshka-style learning facilitates sentence embedding by optimizing embeddings in a nested manner.

5.2 Ablation Study

We conduct ablation studies of the proposed 2DMSE on the standard STS benchmark. The results are presented in Table 2. From the table, we can observe that 2DMSE aided with alignment \mathcal{L}_{align} and last layer learning \mathcal{L}_N^D consistently outperforms other settings. This demonstrates their positive contribution to the models’ performance.

Model	Avg. Spearman’s Correlation
$n = 12, d = 768$	
2DMSE	82.65
w/o alignment \mathcal{L}_{align}	82.57 (-0.08)
w/o last layer \mathcal{L}_N^D	81.31 (-1.34)
$n = 8, d = 512$	
2DMSE	78.02
w/o alignment \mathcal{L}_{align}	77.94 (-0.08)
w/o last layer \mathcal{L}_N^D	76.52 (-1.50)
$n = 6, d = 384$	
2DMSE	75.21
w/o alignment \mathcal{L}_{align}	75.08 (-0.13)
w/o last layer \mathcal{L}_N^D	74.98 (-0.23)
$n = 4, d = 256$	
2DMSE	73.93
w/o alignment \mathcal{L}_{align}	73.69 (-0.24)
w/o last layer \mathcal{L}_N^D	73.00 (-0.93)

Table 2: Ablation study results of 2DMSE on the standard STS benchmark using BERT_{base}. n denotes the number of Transformer layers, and d stands for the embedding dimensions.

Additionally, we notice that, when the last attention layer learning \mathcal{L}_N^D is omitted, performance will decrease significantly. This is likely because the last layer possesses strong language understanding capabilities, enhancing sentence embeddings and potentially improving the performance of sub-attention layers through alignment.

5.3 Efficiency Study

To quantify the efficiency of 2DMSE during the inference stage, we record the time cost for generating embeddings at different layers for the entire STS benchmark. The results are visualized in Table 4a. Meanwhile, we compare the performance on STS benchmarks of different learning strategies using full-capacity embeddings at each layer in Table 4b. The inference time linearly in-

creases with the number of layers. For example, 2DMSE exhibits a $2.0 \times$ theoretical speedup and approximately $\sim 1.46 \times$ real-world speedup when using the middle layer (i.e., layer #6) compared to layer #12. Regarding trade-offs in performance, 2DMSE experiences a score drop of 7.15 using the middle layer’s embedding, whereas MRL and AnglE suffer score reductions of 25.79 and 33.44, respectively.

5.4 Discussion

Effectiveness of Two-Dimensional Matryoshka Learning. When comparing the sentence embedding performance on STS benchmarks using the embedding vectors from all the layers of AnglE (represented by the blue ● line in Figure 3), an unexpected drop is observed as the layers deepen, specifically from layer #5 to layer #8. Decisive improvements are not observed until the deeper layers, from layer #9 to layer #12. In contrast, 2DMSE consistently yields improvements as the layers deepen. We attribute this to the rigidity of using a fixed-depth encoding pipeline, as deep learning models tend to distribute the high-level feature extraction process across all layers, even when it may not be necessary to have as many layers. Thus, matryoshka learning across layers can more effectively utilize the encoding capacity unleashed by the scaling law.

Furthermore, our experiments demonstrate that the proposed 2DMSE, applying matryoshka learning at all layers, brings further improvements over MRL, which applies matryoshka learning only at the last layer. We believe this is because 2DMSE refines all Transformer layers by interpolating coarse-to-fine-grained information across all embedding dimensions. At each layer, information tends to be concentrated at one end while maintaining a long tail at the other end. Consequently, embeddings from 2DMSE are more compact than those learned from normal fine-tuning, facilitating feature extraction in subsequent layers and ultimately improving absolute embedding performance.

Scalability of 2DMSE Model. In our main experiments, we demonstrated the superior scalability of the proposed 2DMSE compared to baselines. To further investigate the scaling of the 2DMSE model, we conducted an experiment where we scaled down the trained $\text{BERT}_{\text{base}}$ ($N = 12, D = 768$) 2DMSE model to $\text{BERT}_{\text{small}}$ ($N = 4, D = 512$) and $\text{BERT}_{\text{tiny}}$ ($N = 12, D = 128$) sizes. We then

compared the performance of these scaled-down models with $\text{BERT}_{\text{small}}$ and $\text{BERT}_{\text{tiny}}$ models trained independently on MultiNLI + NLI. The results, presented in Table 3, show that the scaled 2DMSE consistently outperforms $\text{BERT}_{\text{small}}$ and $\text{BERT}_{\text{tiny}}$, suggesting superior scalability of the 2DMSE model.

With reduced model depth, 2DMSE provides exceptional efficiency and scalability in memory consumption and inference time, with minimal efficiency-vs-accuracy trade-off. One can simply remove the last two or three layers from the original backbone to satisfy deployment constraints.

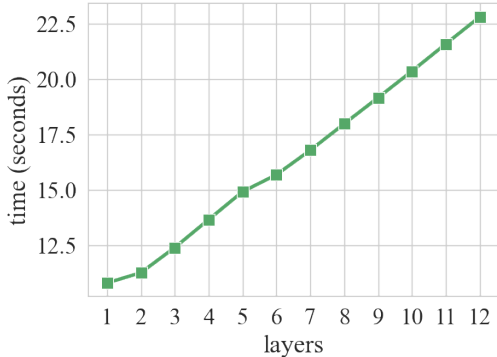
Model ↓	Avg. Spearman’s Correlation	
<i>Small Scale ($n = 4, d = 512$)</i>		
$\text{BERT}_{\text{small}}$	74.01	
MRL w/ $\text{BERT}_{\text{base}}$	54.91	(-19.10)
2DMSE w/ $\text{BERT}_{\text{base}}$	74.46	(+0.35)
<i>Tiny Scale ($n = 2, d = 128$)</i>		
$\text{BERT}_{\text{tiny}}$	69.85	
MRL w/ $\text{BERT}_{\text{base}}$	54.90	(-14.95)
2DMSE w/ $\text{BERT}_{\text{base}}$	71.64	(+1.79)

Table 3: Results of different model scales and their independently trained counterparts. The average Spearman’s correlation of the STS Benchmark serves as the metric. n denotes the number of Transformer layers, and d stands for the embedding dimensions.

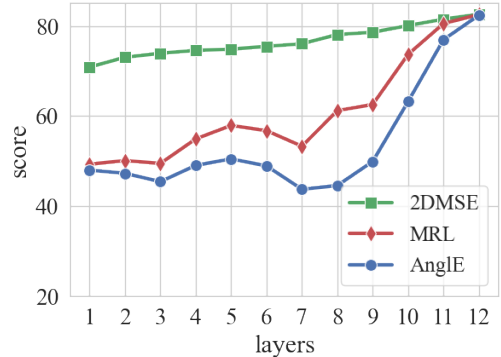
Discussion of Computational Overhead. Here, we compare the proposed 2DMSE with MRL in terms of computational overhead. MRL requires traversing all Transformer layers to produce sentence embeddings, leading to significant computational overhead. The computational complexity of MRL can be seen as $O(N)$, where N is the total number of Transformer attention layers. On the other hand, 2DMSE can reduce computational overhead thanks to its scalable Transformer layer feature. Its computational complexity can be seen as $O(n)$, where $n \leq N$ represents the number of Transformer layers.

6 Conclusion

In this paper, we have proposed a novel sentence embedding model called 2D Matryoshka Sentence Embeddings (2DMSE). 2DMSE offers enhanced scalability by accommodating encoding models of various sizes and capacities. By providing flexibility in the selection of encoding layers and their respective dimensions, our approach can



(a) Inference time *vs* number of layers.



(b) Score on STS *vs* number of layers.

Figure 4: Subfigure (a) illustrates the time taken to use embeddings from different layers to encode the entire STS benchmarks. Subfigure (b) displays the average Spearman's correlation scores of different layers. Both (a) and (b) use an embedding size of 768 and the standard STS benchmark dataset.

adapt to different computational resources and requirements. This scalability empowers researchers and practitioners to efficiently leverage 2DMSE in diverse settings.

Extensive experiments on STS benchmarks have demonstrated that 2DMSE consistently outperforms baselines and exhibits superior scalability, making our approach well-suited for a wide range of downstream applications.

References

Eneko Agirre, Carmen Banea, Claire Cardie, Daniel Cer, Mona Diab, Aitor Gonzalez-Agirre, Weiwei Guo, Iñigo Lopez-Gazpio, Montse Maritxalar, Rada Mihalcea, German Rigau, Larraitz Uria, and Janyce Wiebe. 2015. *SemEval-2015 task 2: Semantic textual similarity, English, Spanish and pilot on interpretability*. In *Proceedings of the 9th International Workshop on Semantic Evaluation (SemEval 2015)*, pages 252–263, Denver, Colorado. Association for Computational Linguistics.

Eneko Agirre, Carmen Banea, Claire Cardie, Daniel Cer, Mona Diab, Aitor Gonzalez-Agirre, Weiwei Guo, Rada Mihalcea, German Rigau, and Janyce Wiebe. 2014. *SemEval-2014 task 10: Multilingual semantic textual similarity*. In *Proceedings of the 8th International Workshop on Semantic Evaluation (SemEval 2014)*, pages 81–91, Dublin, Ireland. Association for Computational Linguistics.

Eneko Agirre, Carmen Banea, Daniel Cer, Mona Diab, Aitor Gonzalez-Agirre, Rada Mihalcea, German Rigau, and Janyce Wiebe. 2016. *SemEval-2016 task 1: Semantic textual similarity, monolingual and cross-lingual evaluation*. In *Proceedings of the 10th International Workshop on Semantic Evaluation (SemEval-2016)*, pages 497–511, San Diego, California. Association for Computational Linguistics.

Eneko Agirre, Daniel Cer, Mona Diab, Iñigo Lopez-Gazpio, and Lucia Specia. 2017. *SemEval-2017 task 1: Semantic textual similarity multilingual and crosslingual focused evaluation*. In *Proceedings of the 11th International Workshop on Semantic Evaluation (SemEval-2017)*, pages 1–14, Vancouver, Canada. Association for Computational Linguistics.

Daniel Cer, Yinfei Yang, Sheng-yi Kong, Nan Hua, Nicole Limtiaco, Rhomni St. John, Noah Constant, Eneko Agirre, Daniel Cer, Mona Diab, and Aitor Gonzalez-Agirre. 2012. *SemEval-2012 task 6: A pilot on semantic textual similarity*. In **SEM 2012: The First Joint Conference on Lexical and Computational Semantics – Volume 1: Proceedings of the main conference and the shared task, and Volume 2: Proceedings of the Sixth International Workshop on Semantic Evaluation (SemEval 2012)*, pages 385–393, Montréal, Canada. Association for Computational Linguistics.

Eneko Agirre, Daniel Cer, Mona Diab, Aitor Gonzalez-Agirre, and Weiwei Guo. 2013. **SEM 2013 shared task: Semantic textual similarity*. In *Second Joint Conference on Lexical and Computational Semantics (*SEM), Volume 1: Proceedings of the Main Conference and the Shared Task: Semantic Textual Similarity*, pages 32–43, Atlanta, Georgia, USA. Association for Computational Linguistics.

Samuel R. Bowman, Gabor Angeli, Christopher Potts, and Christopher D. Manning. 2015. *A large annotated corpus for learning natural language inference*. In *Proceedings of the 2015 Conference on Empirical Methods in Natural Language Processing*, pages 632–642, Lisbon, Portugal. Association for Computational Linguistics.

Fredrik Carlsson, Amaru Cuba Gyllensten, Evangelia Gogoulou, Erik Ylipää Hellqvist, and Magnus Sahlgren. 2020. Semantic re-tuning with contrastive tension. In *International conference on learning representations*.

Daniel Cer, Mona Diab, Eneko Agirre, Iñigo Lopez-Gazpio, and Lucia Specia. 2017. *SemEval-2017 task 1: Semantic textual similarity multilingual and crosslingual focused evaluation*. In *Proceedings of the 11th International Workshop on Semantic Evaluation (SemEval-2017)*, pages 1–14, Vancouver, Canada. Association for Computational Linguistics.

Daniel Cer, Yinfei Yang, Sheng-yi Kong, Nan Hua, Nicole Limtiaco, Rhomni St. John, Noah Constant,

Mario Guajardo-Cespedes, Steve Yuan, Chris Tar, Brian Strope, and Ray Kurzweil. 2018. **Universal sentence encoder for English**. In *Proceedings of the 2018 Conference on Empirical Methods in Natural Language Processing: System Demonstrations*, pages 169–174, Brussels, Belgium. Association for Computational Linguistics.

Yung-Sung Chuang, Rumen Dangovski, Hongyin Luo, Yang Zhang, Shiyu Chang, Marin Soljacic, Shang-Wen Li, Scott Yih, Yoon Kim, and James Glass. 2022. **DiffCSE: Difference-based contrastive learning for sentence embeddings**. In *Proceedings of the 2022 Conference of the North American Chapter of the Association for Computational Linguistics: Human Language Technologies*, pages 4207–4218, Seattle, United States. Association for Computational Linguistics.

Alexis Conneau and Douwe Kiela. 2018. **SentEval: An evaluation toolkit for universal sentence representations**. In *Proceedings of the Eleventh International Conference on Language Resources and Evaluation (LREC 2018)*, Miyazaki, Japan. European Language Resources Association (ELRA).

Alexis Conneau, Douwe Kiela, Holger Schwenk, Loïc Barrault, and Antoine Bordes. 2017. **Supervised learning of universal sentence representations from natural language inference data**. In *Proceedings of the 2017 Conference on Empirical Methods in Natural Language Processing*, pages 670–680, Copenhagen, Denmark. Association for Computational Linguistics.

Jacob Devlin, Ming-Wei Chang, Kenton Lee, and Kristina Toutanova. 2019. **BERT: pre-training of deep bidirectional transformers for language understanding**. In *Proceedings of the 2019 Conference of the North American Chapter of the Association for Computational Linguistics: Human Language Technologies*, pages 4171–4186.

Tianyu Gao, Xingcheng Yao, and Danqi Chen. 2021. **Simcse: Simple contrastive learning of sentence embeddings**. In *Proceedings of the 2021 Conference on Empirical Methods in Natural Language Processing*, pages 6894–6910. Association for Computational Linguistics.

Yunfan Gao, Yun Xiong, Xinyu Gao, Kangxiang Jia, Jinliu Pan, Yuxi Bi, Yi Dai, Jiawei Sun, and Haofen Wang. 2023. **Retrieval-augmented generation for large language models: A survey**. *arXiv preprint arXiv:2312.10997*.

John Giorgi, Osvald Nitski, Bo Wang, and Gary Bader. 2021. **DeCLUTR: Deep contrastive learning for unsupervised textual representations**. In *Proceedings of the 59th Annual Meeting of the Association for Computational Linguistics and the 11th International Joint Conference on Natural Language Processing (Volume 1: Long Papers)*, pages 879–895, Online. Association for Computational Linguistics.

Jay Hegdé. 2008. **Time course of visual perception: coarse-to-fine processing and beyond**. *Progress in neurobiology*, 84(4):405–439.

Yuxin Jiang, Linhan Zhang, and Wei Wang. 2022. **Improved universal sentence embeddings with prompt-based contrastive learning and energy-based learning**. In *Findings of the Association for Computational Linguistics: EMNLP 2022, Abu Dhabi, United Arab Emirates, December 7-11, 2022*, pages 3021–3035. Association for Computational Linguistics.

Jared Kaplan, Sam McCandlish, et al. 2020. **Scaling laws for neural language models**. *arXiv preprint arXiv:2001.08361*.

Aditya Kusupati, Gantavya Bhatt, Aniket Rege, Matthew Wallingford, Aditya Sinha, Vivek Ramanujan, William Howard-Snyder, Kaifeng Chen, Sham Kakade, Prateek Jain, and Ali Farhadi. 2022. **Matyoshka representation learning**. In *Advances in Neural Information Processing Systems*, volume 35, pages 30233–30249. Curran Associates, Inc.

Xianming Li and Jing Li. 2023a. **Angle-optimized text embeddings**. *arXiv preprint arXiv:2309.12871*.

Xianming Li and Jing Li. 2023b. **Deelm: Dependency-enhanced large language model for sentence embeddings**. *arXiv preprint arXiv:2311.05296*.

Xianming Li and Jing Li. 2024. **Generative deduplication for social media data selection**. *arXiv preprint arXiv:2401.05883*.

Marco Marelli, Stefano Menini, Marco Baroni, Luisa Bentivogli, Raffaella Bernardi, and Roberto Zamparelli. 2014. **A SICK cure for the evaluation of compositional distributional semantic models**. In *Proceedings of the Ninth International Conference on Language Resources and Evaluation (LREC'14)*, pages 216–223, Reykjavik, Iceland. European Language Resources Association (ELRA).

Tomás Mikolov, Ilya Sutskever, Kai Chen, Gregory S. Corrado, and Jeffrey Dean. 2013. **Distributed representations of words and phrases and their compositionality**. In *27th Annual Conference on Neural Information Processing Systems 2013.*, pages 3111–3119.

OpenAI. 2022. **Introducing chatgpt**.

Nils Reimers and Iryna Gurevych. 2019. **Sentence-bert: Sentence embeddings using siamese bert-networks**. In *Proceedings of the 2019 Conference on Empirical Methods in Natural Language Processing*, pages 3980–3990. Association for Computational Linguistics.

Hugo Touvron, Louis Martin, Kevin Stone, Peter Albert, Amjad Almahairi, Yasmine Babaei, Nikolay Bashlykov, Soumya Batra, Prajjwal Bhargava, Shruti Bhosale, et al. 2023. **Llama 2: Open foundation and fine-tuned chat models**. *arXiv preprint arXiv:2307.09288*.

Liang Wang, Nan Yang, Xiaolong Huang, Linjun Yang, Rangan Majumder, and Furu Wei. 2023. Improving text embeddings with large language models. *arXiv preprint arXiv:2401.00368*.

Adina Williams, Nikita Nangia, and Samuel Bowman. 2018. [A broad-coverage challenge corpus for sentence understanding through inference](#). In *Proceedings of the 2018 Conference of the North American Chapter of the Association for Computational Linguistics: Human Language Technologies, Volume 1 (Long Papers)*, pages 1112–1122, New Orleans, Louisiana. Association for Computational Linguistics.

Jiahao Xu, Wei Shao, Lihui Chen, and Lemao Liu. 2023. DistillCSE: Distilled contrastive learning for sentence embeddings. In *Findings of the Association for Computational Linguistics: EMNLP 2023*, pages 8153–8165. Association for Computational Linguistics.

Yuanmeng Yan, Rumei Li, Sirui Wang, Fuzheng Zhang, Wei Wu, and Weiran Xu. 2021. Consert: A contrastive framework for self-supervised sentence representation transfer. In *Proceedings of the 59th Annual Meeting of the Association for Computational Linguistics and the 11th International Joint Conference on Natural Language Processing*, pages 5065–5075. Association for Computational Linguistics.

Yan Zhang, Ruidan He, Zuozhu Liu, Kwan Hui Lim, and Lidong Bing. 2020. [An unsupervised sentence embedding method by mutual information maximization](#). In *Proceedings of the 2020 Conference on Empirical Methods in Natural Language Processing (EMNLP)*, pages 1601–1610, Online. Association for Computational Linguistics.

Wenjie Zhuo, Yifan Sun, Xiaohan Wang, Linchao Zhu, and Yi Yang. 2023. [WhitenedCSE: Whitening-based contrastive learning of sentence embeddings](#). In *Proceedings of the 61st Annual Meeting of the Association for Computational Linguistics (Volume 1: Long Papers)*, pages 12135–12148, Toronto, Canada. Association for Computational Linguistics.

A Main Results

The detailed results of Figure 3 are presented in Table 4.

Model	STS12	STS13	STS14	STS15	STS16	STS-B	Sick-R	Avg.
# Layer $n = 1$								
AnglE ($d = 8$)	32.24	39.92	37.80	39.93	45.66	38.48	45.86	39.98
MRL ($d = 8$)	32.21	42.39	39.60	40.18	44.65	40.05	47.25	40.90
2DMSE ($d = 8$)	58.34	60.35	56.99	65.13	58.81	61.66	64.97	60.89
AnglE ($d = 16$)	44.06	47.76	43.39	49.39	53.41	44.34	52.65	47.86
MRL ($d = 16$)	39.93	49.95	45.93	47.35	54.78	46.25	52.80	48.14
2DMSE ($d = 16$)	61.32	66.25	61.35	70.14	63.58	66.90	67.97	65.36
AnglE ($d = 32$)	48.26	49.72	44.03	52.76	53.97	46.48	52.92	49.73
MRL ($d = 32$)	47.33	51.83	46.37	51.37	56.37	47.45	53.15	50.55
2DMSE ($d = 32$)	62.39	68.29	62.89	72.88	67.24	69.17	67.96	67.26
AnglE ($d = 64$)	49.24	47.23	42.65	54.94	56.40	48.35	53.86	50.38
MRL ($d = 64$)	50.49	49.85	45.69	55.95	58.35	50.57	54.16	52.15
2DMSE ($d = 64$)	63.78	68.48	63.15	74.56	68.35	70.35	69.04	68.24
AnglE ($d = 128$)	50.27	48.38	44.29	53.91	56.84	47.92	53.09	50.67
MRL ($d = 128$)	51.43	51.08	47.15	54.72	58.95	49.86	53.55	52.39
2DMSE ($d = 128$)	64.32	69.36	63.61	74.80	69.39	70.74	69.31	68.79
AnglE ($d = 256$)	46.75	47.24	43.13	50.02	55.00	43.92	49.36	47.92
MRL ($d = 256$)	47.55	49.31	45.33	50.81	56.91	45.73	49.81	49.35
2DMSE ($d = 256$)	64.10	69.90	63.27	75.04	69.88	70.20	68.91	68.76
AnglE ($d = 512$)	46.33	44.56	40.17	51.29	52.66	44.03	51.95	47.28
MRL ($d = 512$)	47.95	45.33	41.89	52.60	53.50	46.03	53.07	48.62
2DMSE ($d = 512$)	65.02	70.75	65.41	77.85	70.33	71.30	69.81	70.07
AnglE ($d = 768$)	47.15	45.33	41.25	52.06	53.13	44.79	52.41	48.02
MRL ($d = 768$)	48.66	46.16	42.93	53.37	53.98	46.65	53.55	49.33
2DMSE ($d = 768$)	64.89	70.78	65.34	77.74	70.54	71.30	70.04	70.09
# Layer $n = 2$								
AnglE ($d = 8$)	26.41	37.68	34.70	41.84	46.83	36.67	45.03	38.45
MRL ($d = 8$)	29.58	42.70	37.05	43.20	45.80	39.24	46.68	40.61
2DMSE ($d = 8$)	60.73	62.66	59.75	68.77	60.48	64.29	66.43	63.30
AnglE ($d = 16$)	35.22	45.28	41.20	49.50	52.42	42.78	51.55	45.42
MRL ($d = 16$)	37.61	49.53	44.17	51.17	53.12	46.03	52.24	47.70
2DMSE ($d = 16$)	63.77	67.93	63.96	73.50	65.34	69.01	69.64	67.59
AnglE ($d = 32$)	42.39	46.89	43.10	49.60	54.16	45.07	52.18	47.63
MRL ($d = 32$)	46.31	51.11	45.63	51.78	55.71	47.44	53.36	50.19
2DMSE ($d = 32$)	65.80	70.98	65.93	75.73	69.30	71.05	70.60	69.91
AnglE ($d = 64$)	46.12	51.18	45.17	58.10	59.10	51.09	54.82	52.23
MRL ($d = 64$)	51.33	54.94	49.07	60.30	60.64	54.90	56.36	55.36
2DMSE ($d = 64$)	66.19	72.15	66.83	76.90	70.49	71.94	72.07	70.94
AnglE ($d = 128$)	46.03	50.75	45.26	57.05	59.80	48.54	54.45	51.70
MRL ($d = 128$)	50.30	54.40	49.37	59.59	61.32	52.95	56.39	54.90
2DMSE ($d = 128$)	66.46	72.77	67.40	77.54	71.85	72.65	72.84	71.64
AnglE ($d = 256$)	44.39	49.07	43.65	52.23	57.39	44.65	51.49	48.98

MRL ($d = 256$)	47.33	51.88	46.74	54.53	58.93	48.03	53.00	51.49
2DMSE ($d = 256$)	66.15	73.24	67.36	77.85	72.71	73.00	73.18	71.93
AnglE ($d = 512$)	44.33	45.13	39.26	51.23	52.84	42.96	52.04	46.83
MRL ($d = 512$)	48.28	47.80	42.80	54.25	54.48	46.54	53.93	49.73
2DMSE ($d = 512$)	67.76	73.08	69.30	80.03	73.38	74.25	73.37	73.02
AnglE ($d = 768$)	44.79	45.59	39.98	51.54	53.18	43.67	52.39	47.31
MRL ($d = 768$)	48.62	48.13	43.47	54.53	54.83	47.12	54.29	50.14
2DMSE ($d = 768$)	67.68	73.53	69.17	79.80	73.70	74.21	73.52	73.09
# Layer $n = 3$								
AnglE ($d = 8$)	25.87	35.33	34.69	40.32	45.56	35.79	43.80	37.34
MRL ($d = 8$)	23.52	39.87	36.65	42.11	44.18	34.68	45.98	38.14
2DMSE ($d = 8$)	60.73	61.75	61.37	67.90	62.11	65.01	67.34	63.74
AnglE ($d = 16$)	32.79	43.00	40.69	50.57	51.79	42.05	49.93	44.40
MRL ($d = 16$)	31.63	46.16	42.50	50.85	51.00	42.01	51.92	45.15
2DMSE ($d = 16$)	63.46	68.55	65.52	73.82	67.16	69.95	70.65	68.44
AnglE ($d = 32$)	39.20	45.35	42.12	53.29	54.78	44.62	52.88	47.46
MRL ($d = 32$)	39.73	48.94	43.60	54.28	55.41	45.77	54.61	48.91
2DMSE ($d = 32$)	65.74	72.08	67.72	76.28	70.60	72.06	71.79	70.90
AnglE ($d = 64$)	45.79	49.75	43.31	57.32	58.66	49.40	54.26	51.21
MRL ($d = 64$)	49.82	52.86	46.75	60.49	60.53	53.24	56.47	54.31
2DMSE ($d = 64$)	66.45	73.60	68.75	77.53	71.74	73.08	72.92	72.01
AnglE ($d = 128$)	43.10	47.13	41.10	54.51	58.57	45.55	51.79	48.82
MRL ($d = 128$)	47.55	51.36	45.65	59.33	61.22	51.13	55.06	53.04
2DMSE ($d = 128$)	67.31	74.31	69.21	78.07	72.75	73.82	73.37	72.69
AnglE ($d = 256$)	43.19	46.29	40.87	50.70	56.22	42.34	49.71	47.05
MRL ($d = 256$)	46.75	50.57	45.16	55.27	59.16	48.11	53.15	51.17
2DMSE ($d = 256$)	67.60	74.81	69.30	78.63	73.67	74.65	73.86	73.22
AnglE ($d = 512$)	42.00	42.25	37.23	49.34	52.34	40.89	50.07	44.87
MRL ($d = 512$)	45.88	47.14	42.03	54.43	54.82	45.88	53.39	49.08
2DMSE ($d = 512$)	68.35	74.38	70.41	80.21	74.28	75.73	73.72	73.87
AnglE ($d = 768$)	42.88	42.78	37.95	49.71	52.73	41.78	50.33	45.45
MRL ($d = 768$)	46.67	47.28	42.54	54.72	55.16	46.57	53.55	49.50
2DMSE ($d = 768$)	68.48	74.73	70.21	80.07	74.49	75.73	74.08	73.97
# Layer $n = 4$								
AnglE ($d = 8$)	30.39	37.34	32.51	40.76	46.53	33.32	39.21	37.15
MRL ($d = 8$)	21.68	39.76	34.19	43.94	47.53	31.78	40.00	36.98
2DMSE ($d = 8$)	61.90	63.42	62.02	68.96	62.76	65.77	67.96	64.68
AnglE ($d = 16$)	34.34	46.17	40.84	51.61	51.47	43.94	46.23	44.94
MRL ($d = 16$)	35.84	49.26	45.02	55.65	56.23	46.03	47.12	47.88
2DMSE ($d = 16$)	64.89	69.83	66.36	74.53	68.52	71.18	71.09	69.49
AnglE ($d = 32$)	37.42	48.24	41.58	55.34	55.62	46.00	50.45	47.81
MRL ($d = 32$)	40.99	51.02	44.88	58.37	60.02	49.49	51.84	50.94
2DMSE ($d = 32$)	66.73	73.48	68.47	76.19	71.65	73.30	72.58	71.77
AnglE ($d = 64$)	44.42	50.62	42.45	57.06	57.78	49.80	52.27	50.63

MRL ($d = 64$)	50.17	53.86	47.07	62.08	61.08	55.43	55.48	55.02
2DMSE ($d = 64$)	67.72	74.83	69.54	77.94	72.81	74.11	73.57	72.93
AnglE ($d = 128$)	44.28	48.90	41.88	57.51	59.38	49.58	52.32	50.55
MRL ($d = 128$)	50.44	53.38	47.18	63.38	63.37	55.93	56.38	55.72
2DMSE ($d = 128$)	68.47	75.05	70.04	78.41	73.39	74.70	74.22	73.47
AnglE ($d = 256$)	45.07	49.23	42.48	57.45	59.84	48.79	51.91	50.68
MRL ($d = 256$)	50.44	53.89	48.03	63.01	64.09	55.32	56.11	55.84
2DMSE ($d = 256$)	68.95	75.45	69.98	79.01	74.19	75.40	74.54	73.93
AnglE ($d = 512$)	44.78	45.94	40.20	54.44	56.76	47.07	51.65	48.69
MRL ($d = 512$)	51.34	52.35	46.72	61.16	61.15	55.08	56.56	54.91
2DMSE ($d = 512$)	69.44	75.25	70.97	80.29	74.62	76.40	74.24	74.46
AnglE ($d = 768$)	45.38	46.24	40.73	54.84	57.07	47.49	51.71	49.07
MRL ($d = 768$)	51.68	52.20	46.90	61.24	61.16	55.01	56.44	54.95
2DMSE ($d = 768$)	69.77	75.56	70.80	80.23	74.89	76.45	74.56	74.61
# Layer $n = 5$								
AnglE ($d = 8$)	29.46	40.52	35.44	43.85	46.16	30.69	41.24	38.19
MRL ($d = 8$)	25.81	42.71	36.61	50.08	50.04	36.01	48.81	41.44
2DMSE ($d = 8$)	64.49	63.63	62.30	69.04	63.76	66.43	68.34	65.43
AnglE ($d = 16$)	38.29	47.23	39.62	52.33	48.34	37.06	47.73	44.37
MRL ($d = 16$)	38.18	49.70	43.84	58.91	55.19	43.45	51.77	48.72
2DMSE ($d = 16$)	67.51	70.51	67.08	74.60	69.42	71.79	71.09	70.29
AnglE ($d = 32$)	38.13	48.52	40.71	56.08	54.90	41.73	53.54	47.66
MRL ($d = 32$)	41.40	52.11	45.72	61.31	60.16	49.23	57.34	52.47
2DMSE ($d = 32$)	68.16	73.89	69.29	75.93	72.00	73.54	72.44	72.18
AnglE ($d = 64$)	43.72	50.22	42.17	58.35	57.21	47.65	55.44	50.68
MRL ($d = 64$)	49.75	55.55	48.85	64.67	61.99	56.96	58.54	56.62
2DMSE ($d = 64$)	68.98	74.99	70.10	77.61	73.36	74.35	73.69	73.30
AnglE ($d = 128$)	42.82	50.30	42.01	58.98	59.50	48.06	55.64	51.04
MRL ($d = 128$)	50.39	56.18	49.34	65.65	64.30	58.77	59.73	57.77
2DMSE ($d = 128$)	69.24	75.59	70.70	78.02	74.10	75.05	74.29	73.86
AnglE ($d = 256$)	41.87	52.18	42.69	59.01	60.42	46.93	54.83	51.13
MRL ($d = 256$)	49.30	57.49	49.84	65.60	65.60	57.55	59.22	57.80
2DMSE ($d = 256$)	69.49	76.07	70.76	78.96	74.87	75.95	74.48	74.37
AnglE ($d = 512$)	44.88	49.86	41.57	57.19	58.65	45.63	54.58	50.34
MRL ($d = 512$)	53.46	56.87	49.66	64.76	64.13	57.73	59.50	58.02
2DMSE ($d = 512$)	69.76	75.66	71.64	80.03	75.14	76.61	73.98	74.69
AnglE ($d = 768$)	44.84	50.22	41.77	57.54	58.84	45.74	54.64	50.51
MRL ($d = 768$)	53.08	56.95	49.61	64.85	64.22	57.40	59.49	57.94
2DMSE ($d = 768$)	70.12	76.01	71.45	80.08	75.43	76.75	74.40	74.89
# Layer $n = 6$								
AnglE ($d = 8$)	28.48	42.25	34.83	40.93	43.27	29.63	41.93	37.33
MRL ($d = 8$)	28.02	40.18	36.33	51.92	49.60	36.53	50.40	41.85
2DMSE ($d = 8$)	64.65	64.15	63.02	69.65	63.99	67.01	68.34	65.83
AnglE ($d = 16$)	35.74	46.28	38.05	50.36	45.00	34.08	47.19	42.39

MRL ($d = 16$)	36.36	47.59	41.05	57.14	52.20	40.97	52.79	46.87
2DMSE ($d = 16$)	67.80	71.56	67.91	74.52	69.61	72.79	71.47	70.81
AnglE ($d = 32$)	34.78	48.15	38.93	52.59	52.01	38.14	52.57	45.31
MRL ($d = 32$)	38.46	50.02	42.32	58.25	57.30	45.18	57.08	49.80
2DMSE ($d = 32$)	68.69	75.42	70.47	76.17	72.74	74.85	72.92	73.04
AnglE ($d = 64$)	40.02	49.26	39.91	55.29	55.20	44.21	53.73	48.23
MRL ($d = 64$)	46.77	53.69	46.23	61.57	60.01	53.29	57.38	54.13
2DMSE ($d = 64$)	69.52	76.74	71.25	77.92	74.26	76.01	74.18	74.27
AnglE ($d = 128$)	39.84	50.11	40.31	56.86	57.52	45.48	54.88	49.29
MRL ($d = 128$)	47.09	55.48	47.40	62.55	62.70	55.97	59.22	55.77
2DMSE ($d = 128$)	69.70	77.20	71.92	78.39	74.77	76.59	74.25	74.69
AnglE ($d = 256$)	38.08	51.23	40.61	56.61	58.39	43.86	53.71	48.93
MRL ($d = 256$)	44.91	56.81	47.94	62.63	64.11	54.68	59.13	55.74
2DMSE ($d = 256$)	70.00	77.72	72.20	79.38	75.28	77.38	74.09	75.15
AnglE ($d = 512$)	42.91	48.50	39.62	56.12	57.36	43.50	53.14	48.74
MRL ($d = 512$)	50.92	56.20	48.09	63.95	63.31	55.88	59.00	56.76
2DMSE ($d = 512$)	70.75	76.91	72.84	80.40	75.32	77.84	73.36	75.35
AnglE ($d = 768$)	42.84	48.97	39.89	56.34	57.47	43.81	53.40	48.96
MRL ($d = 768$)	50.59	56.46	48.19	63.74	63.49	55.85	59.15	56.78
2DMSE ($d = 768$)	70.87	77.26	72.69	80.41	75.56	78.04	73.65	75.50

# Layer $n = 7$								
AnglE ($d = 8$)	17.23	40.98	32.35	39.12	41.39	26.25	40.54	33.98
MRL ($d = 8$)	23.71	41.64	34.63	45.35	47.47	32.45	45.74	38.71
2DMSE ($d = 8$)	64.42	63.40	63.22	70.03	64.34	67.94	68.82	66.02
AnglE ($d = 16$)	21.76	42.24	33.69	43.24	45.65	28.69	41.71	36.71
MRL ($d = 16$)	27.36	45.74	37.19	48.37	51.68	34.14	47.43	41.70
2DMSE ($d = 16$)	67.65	70.93	68.19	74.17	69.94	74.05	72.41	71.05
AnglE ($d = 32$)	16.48	46.16	32.34	41.39	52.90	28.63	46.37	37.75
MRL ($d = 32$)	27.94	48.58	38.10	48.56	56.44	36.58	50.84	43.86
2DMSE ($d = 32$)	68.78	75.10	70.96	76.22	72.59	75.98	73.99	73.37
AnglE ($d = 64$)	30.52	47.70	35.52	48.37	53.99	37.54	48.36	43.14
MRL ($d = 64$)	38.91	52.15	42.77	54.97	58.84	46.25	53.19	49.58
2DMSE ($d = 64$)	70.04	76.63	71.82	78.05	74.25	76.85	75.16	74.69
AnglE ($d = 128$)	30.77	47.75	35.43	49.94	54.96	37.41	48.81	43.58
MRL ($d = 128$)	40.50	54.16	44.01	56.51	60.75	48.22	53.77	51.13
2DMSE ($d = 128$)	70.47	77.34	72.67	78.83	74.90	77.64	75.42	75.32
AnglE ($d = 256$)	27.84	48.57	35.28	48.57	55.05	35.41	48.19	42.70
MRL ($d = 256$)	36.14	55.30	43.89	55.23	61.62	45.86	53.68	50.25
2DMSE ($d = 256$)	70.62	77.73	72.74	79.67	75.35	78.19	75.33	75.66
AnglE ($d = 512$)	35.35	45.40	35.31	50.22	53.78	36.90	48.42	43.63
MRL ($d = 512$)	46.77	53.88	46.21	59.74	61.26	51.02	54.45	53.33
2DMSE ($d = 512$)	71.66	77.30	73.37	81.01	75.47	78.57	74.84	76.03
AnglE ($d = 768$)	35.08	45.78	35.57	50.49	53.83	36.96	48.59	43.76
MRL ($d = 768$)	45.87	54.56	46.34	59.46	61.50	50.96	54.61	53.33

2DMSE ($d = 768$)	71.57	77.64	73.29	80.92	75.63	78.65	74.93	76.09
# Layer $n = 8$								
AnglE ($d = 8$)	11.53	38.60	32.96	41.79	38.23	24.76	43.95	33.12
MRL ($d = 8$)	37.35	46.52	39.84	46.34	51.98	43.43	51.31	45.25
2DMSE ($d = 8$)	64.24	65.14	63.67	70.42	66.21	68.87	69.04	66.80
AnglE ($d = 16$)	21.80	41.79	33.74	44.52	45.35	30.67	45.88	37.68
MRL ($d = 16$)	40.91	51.06	42.62	50.55	57.65	46.04	53.56	48.91
2DMSE ($d = 16$)	67.52	71.78	68.82	74.68	71.27	74.52	73.13	71.67
AnglE ($d = 32$)	21.15	46.99	34.47	42.67	52.15	32.00	49.24	39.81
MRL ($d = 32$)	44.44	55.63	45.75	52.72	62.59	50.08	56.88	52.58
2DMSE ($d = 32$)	69.19	76.04	71.99	76.98	74.27	76.98	74.94	74.34
AnglE ($d = 64$)	33.96	49.19	37.35	49.08	55.31	40.49	51.20	45.23
MRL ($d = 64$)	53.37	58.65	49.70	59.30	65.70	58.12	59.77	57.80
2DMSE ($d = 64$)	70.92	77.86	73.25	79.10	76.19	78.38	76.12	75.97
AnglE ($d = 128$)	32.35	50.38	37.86	51.07	56.60	40.41	51.67	45.76
MRL ($d = 128$)	55.46	60.59	51.38	62.30	67.98	61.03	61.11	59.98
2DMSE ($d = 128$)	71.50	78.91	74.31	80.46	76.84	79.70	76.71	76.92
AnglE ($d = 256$)	29.43	50.44	37.43	49.84	56.44	37.95	51.12	44.66
MRL ($d = 256$)	52.09	60.77	51.49	61.04	68.14	60.07	61.15	59.25
2DMSE ($d = 256$)	71.73	79.54	74.73	81.28	77.46	80.55	76.91	77.46
AnglE ($d = 512$)	35.70	46.06	35.63	50.10	54.54	37.94	49.47	44.21
MRL ($d = 512$)	58.02	59.07	52.68	65.13	67.73	63.13	60.73	60.93
2DMSE ($d = 512$)	72.95	79.05	75.94	82.64	77.77	81.43	76.43	78.03
AnglE ($d = 768$)	35.43	46.69	36.10	50.80	54.96	38.20	50.03	44.60
MRL ($d = 768$)	57.56	59.83	53.01	65.31	68.12	63.57	61.19	61.23
2DMSE ($d = 768$)	72.93	79.57	75.93	82.52	77.92	81.47	76.60	78.13
# Layer $n = 9$								
AnglE ($d = 8$)	29.60	36.46	35.65	50.23	40.42	32.26	47.43	38.86
MRL ($d = 8$)	47.80	51.30	47.09	52.16	55.71	50.79	54.38	51.32
2DMSE ($d = 8$)	64.21	65.65	64.37	71.21	66.51	69.43	68.43	67.12
AnglE ($d = 16$)	37.21	39.61	37.10	51.63	48.19	37.87	51.21	43.26
MRL ($d = 16$)	50.95	55.35	49.99	55.93	60.89	52.87	56.46	54.63
2DMSE ($d = 16$)	67.79	72.51	69.61	75.51	71.74	74.80	73.09	72.15
AnglE ($d = 32$)	31.84	45.55	38.22	50.90	55.63	38.32	53.19	44.81
MRL ($d = 32$)	51.57	60.03	52.50	57.82	64.91	54.98	58.44	57.18
2DMSE ($d = 32$)	69.73	77.13	72.87	77.94	74.85	77.84	74.55	74.99
AnglE ($d = 64$)	43.08	49.07	42.22	56.56	56.83	46.79	55.11	49.95
MRL ($d = 64$)	56.27	61.88	55.23	62.65	66.14	59.41	60.53	60.30
2DMSE ($d = 64$)	71.60	79.33	74.48	80.00	76.63	79.35	75.82	76.74
AnglE ($d = 128$)	43.19	51.14	44.57	57.80	58.07	48.17	55.48	51.20
MRL ($d = 128$)	57.58	63.10	56.67	65.58	67.11	61.29	61.09	61.77
2DMSE ($d = 128$)	71.89	80.28	75.31	81.06	77.35	80.58	76.26	77.53
AnglE ($d = 256$)	41.84	52.02	45.29	57.55	57.72	47.88	54.91	51.03
MRL ($d = 256$)	56.16	63.13	57.33	65.62	67.42	61.87	61.29	61.83

2DMSE ($d = 256$)	72.09	80.91	75.82	81.92	77.87	81.34	76.83	78.11
AnglE ($d = 512$)	44.49	46.94	41.85	56.22	55.95	46.54	53.24	49.32
MRL ($d = 512$)	59.11	60.71	57.40	67.57	66.99	63.45	60.10	62.19
2DMSE ($d = 512$)	72.82	80.32	77.06	82.99	78.00	81.90	76.39	78.50
AnglE ($d = 768$)	44.61	47.61	42.59	57.31	56.58	46.96	53.92	49.94
MRL ($d = 768$)	58.84	61.52	57.88	68.06	67.39	63.83	60.70	62.60
2DMSE ($d = 768$)	72.78	80.83	77.04	83.04	78.34	81.96	76.47	78.64
# Layer $n = 10$								
AnglE ($d = 8$)	50.59	50.23	46.91	56.53	45.64	47.25	58.33	50.78
MRL ($d = 8$)	58.56	62.83	59.16	59.58	62.75	63.10	62.28	61.18
2DMSE ($d = 8$)	63.12	67.89	65.34	70.73	67.28	69.94	68.39	67.53
AnglE ($d = 16$)	56.74	57.25	49.42	59.66	55.61	55.47	63.50	56.81
MRL ($d = 16$)	63.12	68.44	63.53	65.26	67.39	66.53	65.03	65.61
2DMSE ($d = 16$)	67.71	75.09	70.97	75.99	72.07	75.04	73.01	72.84
AnglE ($d = 32$)	53.35	63.09	51.85	61.06	61.22	57.70	63.73	58.86
MRL ($d = 32$)	66.13	73.22	66.47	69.28	71.60	70.78	66.51	69.14
2DMSE ($d = 32$)	70.44	79.56	74.66	78.50	75.44	78.60	74.52	75.96
AnglE ($d = 64$)	59.31	65.90	58.30	66.09	63.16	64.85	65.95	63.37
MRL ($d = 64$)	68.15	75.91	69.42	72.24	73.24	73.94	67.92	71.55
2DMSE ($d = 64$)	72.00	81.70	76.65	80.58	77.42	80.47	76.25	77.87
AnglE ($d = 128$)	58.77	67.59	59.50	66.81	64.16	66.37	66.18	64.20
MRL ($d = 128$)	68.16	77.85	70.52	73.68	74.58	75.65	68.73	72.74
2DMSE ($d = 128$)	72.42	82.82	77.62	81.68	78.42	81.89	77.05	78.84
AnglE ($d = 256$)	57.77	67.45	60.04	66.92	64.07	66.28	66.09	64.09
MRL ($d = 256$)	67.86	78.18	71.36	74.78	74.70	76.62	69.35	73.26
2DMSE ($d = 256$)	72.13	83.32	78.08	82.40	79.08	82.63	77.83	79.35
AnglE ($d = 512$)	59.07	63.21	57.79	66.32	62.74	64.23	65.01	62.62
MRL ($d = 512$)	69.59	76.81	72.34	75.98	74.30	76.43	67.74	73.31
2DMSE ($d = 512$)	73.44	83.47	79.38	83.68	79.29	83.13	77.63	80.00
AnglE ($d = 768$)	59.43	64.16	58.38	67.23	63.19	64.82	65.53	63.25
MRL ($d = 768$)	69.55	77.57	72.54	76.55	74.63	76.88	68.37	73.73
2DMSE ($d = 768$)	73.33	83.85	79.31	83.70	79.52	83.30	77.83	80.12
# Layer $n = 11$								
AnglE ($d = 8$)	55.75	62.27	56.75	62.93	56.41	57.73	64.89	59.53
MRL ($d = 8$)	63.51	69.66	65.51	67.15	67.22	70.84	66.41	67.19
2DMSE ($d = 8$)	63.51	69.30	65.99	69.63	67.73	70.02	68.64	67.83
AnglE ($d = 16$)	65.21	67.76	61.99	69.40	65.90	68.81	70.69	67.11
MRL ($d = 16$)	68.38	76.16	71.63	74.40	73.04	76.45	70.24	72.90
2DMSE ($d = 16$)	68.57	76.40	72.13	76.04	73.23	75.65	73.23	73.61
AnglE ($d = 32$)	69.74	74.26	67.83	73.26	73.12	75.84	75.39	72.78
MRL ($d = 32$)	71.77	80.72	75.25	78.82	77.03	80.18	72.59	76.62
2DMSE ($d = 32$)	71.51	81.37	76.21	79.12	77.09	79.76	75.39	77.21
AnglE ($d = 64$)	71.70	77.12	71.90	76.61	75.53	78.57	77.08	75.50
MRL ($d = 64$)	73.51	82.87	77.59	80.96	79.02	81.67	74.44	78.58

2DMSE ($d = 64$)	73.32	83.57	78.45	81.41	79.21	81.90	77.28	79.31
AnglE ($d = 128$)	70.75	78.68	73.00	78.64	76.62	80.09	77.54	76.47
MRL ($d = 128$)	73.25	84.11	78.43	82.31	79.97	82.91	75.63	79.52
2DMSE ($d = 128$)	73.53	84.61	79.39	82.84	80.05	83.11	78.26	80.26
AnglE ($d = 256$)	70.94	78.83	73.81	80.52	76.60	80.55	77.46	76.96
MRL ($d = 256$)	73.03	84.26	79.07	83.68	80.42	83.54	76.46	80.07
2DMSE ($d = 256$)	73.11	84.80	79.85	84.00	80.75	83.71	79.07	80.76
AnglE ($d = 512$)	72.10	74.66	73.83	80.96	75.95	80.65	75.34	76.21
MRL ($d = 512$)	74.57	83.17	80.41	84.11	80.39	83.41	74.45	80.07
2DMSE ($d = 512$)	74.50	84.83	81.36	85.36	80.83	84.26	78.32	81.35
AnglE ($d = 768$)	72.73	76.37	74.39	81.70	76.51	81.09	76.13	76.99
MRL ($d = 768$)	74.70	84.12	80.66	84.72	80.70	83.75	75.36	80.57
2DMSE ($d = 768$)	74.32	85.39	81.39	85.49	81.04	84.48	78.77	81.55
# Layer $n = 12$								
AnglE ($d = 8$)	57.45	67.73	60.77	67.17	60.64	62.19	65.98	63.13
MRL ($d = 8$)	64.42	71.68	67.66	70.87	68.60	72.26	68.29	69.11
2DMSE ($d = 8$)	63.04	69.74	67.01	72.14	68.42	70.69	69.49	68.65
AnglE ($d = 16$)	65.03	75.86	68.69	73.76	70.58	72.81	72.37	71.30
MRL ($d = 16$)	70.48	79.16	74.10	78.55	74.84	78.99	73.42	75.65
2DMSE ($d = 16$)	69.60	77.91	74.29	78.88	74.92	77.37	75.22	75.46
AnglE ($d = 32$)	71.87	80.53	73.55	77.23	77.16	79.44	76.11	76.56
MRL ($d = 32$)	73.63	83.42	77.70	82.55	78.00	82.23	75.92	79.06
2DMSE ($d = 32$)	72.63	83.11	78.49	82.26	78.62	81.49	77.48	79.15
AnglE ($d = 64$)	73.20	82.90	77.08	81.16	80.42	82.30	79.06	79.45
MRL ($d = 64$)	74.89	85.06	79.65	84.19	80.13	83.58	77.72	80.75
2DMSE ($d = 64$)	74.35	84.99	80.45	84.18	80.67	83.74	78.99	81.05
AnglE ($d = 128$)	74.10	84.18	78.52	83.13	81.56	84.12	80.36	80.85
MRL ($d = 128$)	75.29	85.97	80.54	85.57	80.94	84.51	78.41	81.60
2DMSE ($d = 128$)	74.68	85.88	81.22	85.53	81.51	84.76	79.67	81.89
AnglE ($d = 256$)	74.17	84.98	79.38	85.07	81.89	84.90	80.85	81.61
MRL ($d = 256$)	75.08	86.20	81.07	86.34	81.30	84.84	79.00	81.98
2DMSE ($d = 256$)	74.52	86.17	81.72	86.06	81.93	85.21	79.97	82.23
AnglE ($d = 512$)	75.12	84.86	80.50	86.23	82.44	85.76	80.72	82.23
MRL ($d = 512$)	75.90	86.57	81.86	86.72	81.72	85.57	79.17	82.50
2DMSE ($d = 512$)	75.09	86.49	82.29	86.46	82.02	85.73	80.04	82.59
AnglE ($d = 768$)	75.26	85.61	80.64	86.36	82.51	85.64	80.99	82.43
MRL ($d = 768$)	75.72	86.79	81.89	86.91	81.74	85.50	79.44	82.57
2DMSE ($d = 768$)	75.00	86.69	82.30	86.50	82.09	85.79	80.18	82.65

Table 4: Detailed STS Benchmark results of scalable sentence embeddings. BERT_{base} serves as the backbone for all models.